Quartz crystal microbalance and spectroscopy measurements for acid doping in polyaniline films

2008 Sci. Technol. Adv. Mater. 9 015007

(http://iopscience.iop.org/1468-6996/9/1/015007)

IOP PUBLISHING SCIENCE AND TECHNOLOGY OF ADVANCED MATERIALS

Sci. Technol. Adv. Mater. **9** (2008) 015007 (10pp) doi:10.1088/1468-6996/9/1/015007

Quartz crystal microbalance and spectroscopy measurements for acid doping in polyaniline films

Mohamad M Ayad and Eman A Zaki

Department of Chemistry, Faculty of Science, University of Tanta, Tanta, Egypt

E-mail: mayad12000@yahoo.com

Received 28 June 2007
Accepted for publication 11 October 2007
Published 13 March 2008
Online at stacks.iop.org/STAM/9/015007

Abstract

We investigated the doping of thin polyaniline (PANI) films, prepared by the chemical oxidation of aniline, with different acids. The initial step in the investigation is the preparation of PANI films from aqueous hydrochloric acid solution. This is followed by dedoping with ammonia to obtain a PANI base, which is subsequently doped with strong acids (e.g. hydrochloric, sulfuric, phosphoric and trichloroacetic acids) and with a weak acid (acetic acid). The dopant weight fraction (***w***), which is connected with the gain of mass during the doping of PANI, was determined *in situ* using a quartz crystal microbalance (QCM). The behavior of PANI upon doping with different anions derived from strong acids indicates that both proton and the anion uptake into the polymer chains occur sharply, rapidly, completely, and reversibly. However the uptake in the case in acetic acid is characterized by slow diffusion. The doping was studied at different concentrations of acetic acid. A second cycle of dedoping–redoping was also performed. The kinetics of the doping reaction is dominated by Fickian diffusion kinetics. The diffusion coefficients (D) of the dopant ions into the PANI chains were determined using the QCM and by UV–Vis absorption spectroscopy in the range of $(0.076–1.64) \times 10^{-15}$ cm^2 s^{-1}. It was found that D in the second cycle of doping is larger than that evaluated from the first cycle of doping for high concentrations of acetic acid. D for the diffusion and for the dopant ion expulsion from the PANI chains was also determined during the redoping process. It was found that D for acetic acid ions in the doping process is larger than that calculated for the dedoping process.

Keywords: diffusion, acid doping, polyaniline film, thin film, quartz crystal microbalance

1. Introduction

Polymers containing conjugating π-electron systems such as polyaniline (PANI), polythiophene and polypyrrole have been well known for many years [1]. PANI has attracted considerable attention because of its good environmental stability, redox reversibility and electrical conductivity. These properties indicate possible applications in battery electrodes [2, 3], electrochromic devices [4, 5], photoelectric cells [6, 7], light-emitting diodes [8] and biosensors [9, 10].

Aniline polymerization in an acidic aqueous medium yields protonated PANI [11, 12]. During the polymerization, the PANI-chain propagation results in the formation of the most conductive form of PANI, the emeraldine salt (ES). Protonated PANI may be converted to the corresponding emeraldine base (EB) by treatment with an alkali solution, or by rinsing with a large excess of water [11, 13], (see schemes 1(a) and (b)). Imine sites of the EB form are easily protonated, with a distinctive insulator–conductor transition induced by the appearance of polarons in the lattice, while the number of π-electrons remains constant. As a consequence, new optical conducting and paramagnetic properties appear in doped PANI, particularly in the ES [14, 15].

The conductivity of PANI is closely related to the redox state of the polymer, the pH of the working medium and the

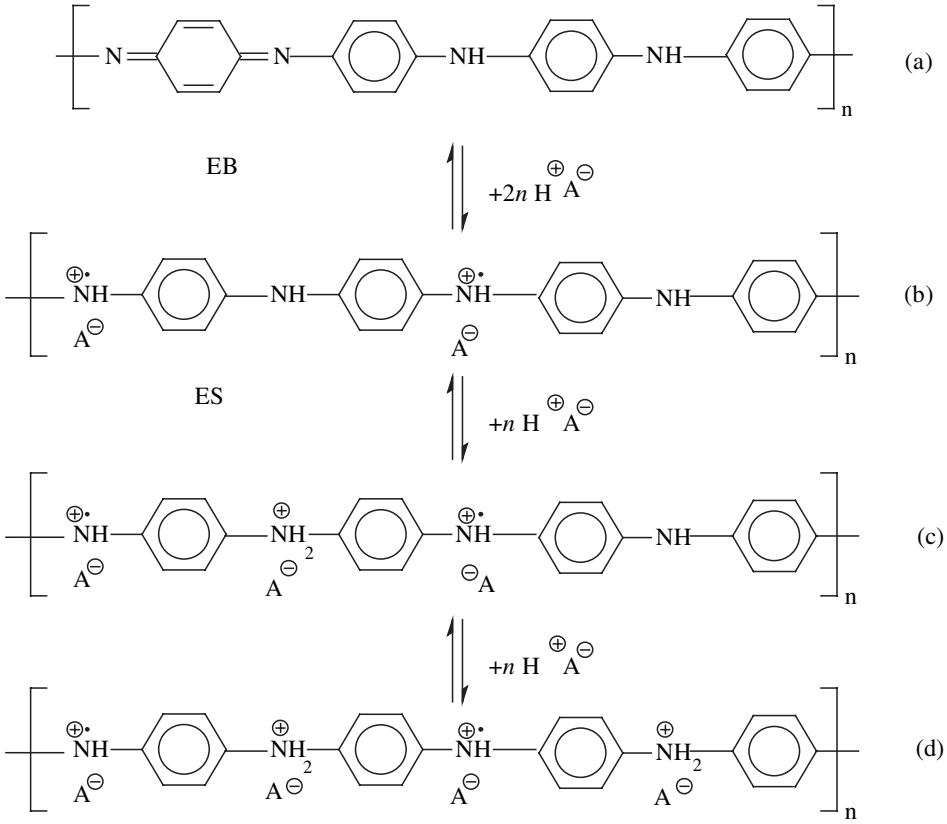

Scheme 1. (a) EB, (b) EB is doped on the imine nitrogens with acid to yield ES. Further doping of amine nitrogens (c) and (d).

type of dopant anion [16]. The type of dopant anion affects the stability of the electrical conductivity of the polymer at various temperatures and atmospheric conditions [17]. The type of dopant anion is also known to affect the polymerization kinetics and the yield of polymer in the electrochemical polymerization of aniline [18, 19].

The redoping and dedoping processes shown in schemes (a) and (b) are assumed to accompany ion migration out of or into the polymer film. Therefore, the mass changes in PANI films resulting from these processes provide direct information concerning the dopant weight fraction (***w***). Therefore, the piezoelectric quartz crystal microbalance (QCM) was applied to determine ***w*** for PANI film deposited onto the surface of a quartz crystal by Ayad *et al* [20]. This method also provides the possibility of following *in situ* small mass changes induced by the interaction between a dopant solution and PANI [21, 22]. Such mass changes are extracted from the shift in resonant frequency of the oscillating quartz crystal. Accordingly, the decrease in mass, resulting from dedoping from a film supported on the quartz crystal, leads to an increase in the resonant frequency [20].

Since thin PANI films have technological importance for numerous applications [2–12], understanding the effects of the interface on the dynamics of these films is essential for their application in future technology. In this work, we quantify the doping process for PANI with different strong acids (hydrochloric, sulfuric, phosphoric and trichloroacetic acids) and a weak acid (acetic acid) using a QCM. The kinetics of the doping process in the case of acetic acid was traced using two independent methods, QCM analysis and UV–Vis absorption spectroscopy. In addition, the kinetics of the dedoping process of acetic acid ions was determined. The diffusion coefficient (D) in both processes was calculated and discussed. The PANI film was synthesized through the chemical oxidation of aniline and characterized using the QCM.

2. Experimental

Aniline (ADWIC, Egypt) was purified by vacuum distillation, and ammonium peroxydisulfate (APS) (WINLAB) was used as received and was stored at 4 °C before the use. Ammonium hydroxide (ADWIC, Egypt), acetic acid (Fisher), hydrochloric acid (ADWIC, Egypt), trichloroacetic acid (Aldrich) and sulfuric acid (Fisher) were all used as received.

In a typical example of PANI preparation, 250 ml of 0.03 M aniline and 0.1 M HCl solution was added to 250 ml of 0.015 M APS solution and 0.1 M HCl. The APS-to-aniline molar ratio after mixing was 0.5. These solutions were added in a polypropylene container, which served as the reaction vessel. A hole had been previously cut in the cap of the container and a 5 MHz AT-cut quartz crystal, one inch in diameter, had been fixed with silicon rubber (RTV) in this hole. This resonator formed the frequency-determining element of an electronic oscillator. Once the reactants were introduced into the vessel, the film grew on the gold electrode of the QCM. The frequency was measured using a GW frequency counter, Model GFC-8055G. Details

of the apparatus design and the procedure are described in earlier studies [23–25]. The mass per unit area of the PANI film, $m'(\mathrm{g\,cm^{-2}})$, grown on the gold surface of the crystal, was determined from the change in the crystal resonance frequency. The frequency decreases linearly with increasing mass deposited on the electrode. The time dependence of frequency was recorded at room temperature (23–24 °C) for each solution. The relation between the frequency change Δf and m' is well known from the work of Sauerbrey [26] and is given by

$$\Delta f = -(2 f_0^2/\sqrt{\rho_Q \mu_Q})\, m', \qquad (1)$$

where f_0 (in Hz) is the natural frequency of the quartz crystal, ρ_Q is the quartz density ($2.649\,\mathrm{g\,cm^{-3}}$), and μ_Q is the shear modulus ($2.947 \times 10^{11}\,\mathrm{dyne\,cm^{-2}}$).

When the QCM is used in an aqueous solution, equation (1) cannot be simply adopted due to the effects of interfacial liquid properties such as viscosity, density and conductivity [27, 28]. It is, however, known that equation (1) can be used for solution systems under specific conditions where the effect of the viscoelasticity of the polymer is negligible [29, 30]. In our experiments, a linear relationship was observed between the change in mass and frequency shift of the QCM both in air and in aqueous solution. Thus, the Sauerbrey equation can be applied to the aqueous solution system under study [27, 28]. Also, since we are dealing with dilute reactant solutions, the variations of viscosity and liquid density were assumed to be negligible during the experiment; hence, the change in frequency due to these effects can be considered constant [28].

The ES film formed after the polymerization was rinsed with the acid solution constituting the reaction medium. The dedoping process was performed by exposure of the film to 0.1 M ammonia solution to give the EB film. The mass loss due to the dedoping process was determined by calculating the increase in the frequency of the PANI-coated quartz crystal. The EB film was then redoped by exposing the film to the acid medium to produce another ES film. The mass gain due to the redoping process was determined by calculating the decrease in the frequency of the PANI-coated quartz crystal.

The thickness of the films was estimated using four samples by measuring the optical absorption as described by Ayad and Shenashin [31].

3. Results and discussion

3.1. Doping of PANI with strong acids

The doping processes for PANI films with 0.1 M hydrochloric, sulfuric and phosphoric acids and with 0.5 M trichloroacetic were studied using the QCM. Doping the PANI film with sulfuric acid was investigated in detail as an example.

Plots of the frequency change due to PANI film deposition on the electrode of the QCM as a function of polymerization time are shown in figure 1. The initially deposited PANI must nucleate on the gold surface, giving rise to a rather slow deposition rate. Following this induction period, the rate of deposition is observed to increase and then to decrease and the frequency attains a steady state once the deposition has finished. The decrease in the deposition rate towards the end of the deposition is due to the depletion of either the oxidant or the monomer or both. The polymerization in the depletion period ends with the formation of *in situ* doped PANI film, which is denoted as ES. *In situ* doping occurs due to the presence of sulfuric acid, constituting the reaction medium and also generated from the reduction of APS. The ES film was dedoped with 0.1 M ammonia solution to give an EB film of frequency f_{EB}, as shown in figure 2(a).

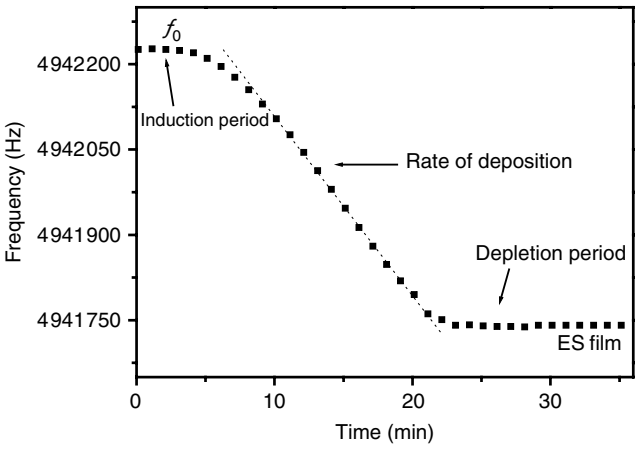

Figure 1. Frequency change due to PANI film deposition onto the gold electrode of the QCM as a function of polymerization time.

The EB film was redoped to form another ES(1) film by exposure to 0.1 M sulfuric acid. It can be seen that the redoping process, i.e. the dopant anion uptake, occurred immediately. The value of the frequency change in comparison with the frequency change due to the ES(1) film formation $\Delta f_{(1)}$ gives $\boldsymbol{w}$ for acid in protonated PANI [20]. Suppose that f_0 is the frequency at zero time of polymerization in figure 1 and $f_{\mathrm{ES}(1)}$ is the frequency of the ES(1) film after redoping the EB film, then the frequency change $\Delta f_{(1)} = f_0 - f_{\mathrm{ES}(1)}$, can be calculated, and it corresponds to the mass of the ES(1) film (1914 Hz). The frequency change due to the redoping (mass gain) is $f_{\mathrm{EB}} - f_{\mathrm{ES}(1)} = 383\,\mathrm{Hz}$. Consequently, the value of $\boldsymbol{w}$ as a percentage during the redoping process is $(383/1914) \times 100 = 20\,\mathrm{wt.\%}$. The ES(1) film was then dedoped to form another EB(1) film by exposure to 0.1 M ammonia solution, see figure 2(a). The dedoping process, i.e. the dopant anion expulsion, occurred immediately. This process represents the first cycle of redoping.

The EB film was redoped to form another ES(1) film by exposure to 0.1 M sulfuric acid solution. The latter film was then exposed to 0.1 M ammonia and 0.1 M sulfuric acid solution to form EB(1) and ES(2) films, respectively, as shown in figure 2(a). This process represents the second cycle of redoping. It can be seen that the uptake and expulsion processes also occurred immediately. In a similar way as for the first redoping process, the value of w associated with the ES(2) film was calculated and is equal to 19 wt.%. This is close to the value calculated for the first redoping cycle. The present results for $\boldsymbol{w}$ suggest that sulfate counterions (scheme 1(b), $\mathrm{A^-} = 1/2\mathrm{SO_4^{2-}}$) were present in PANI [20, 32].

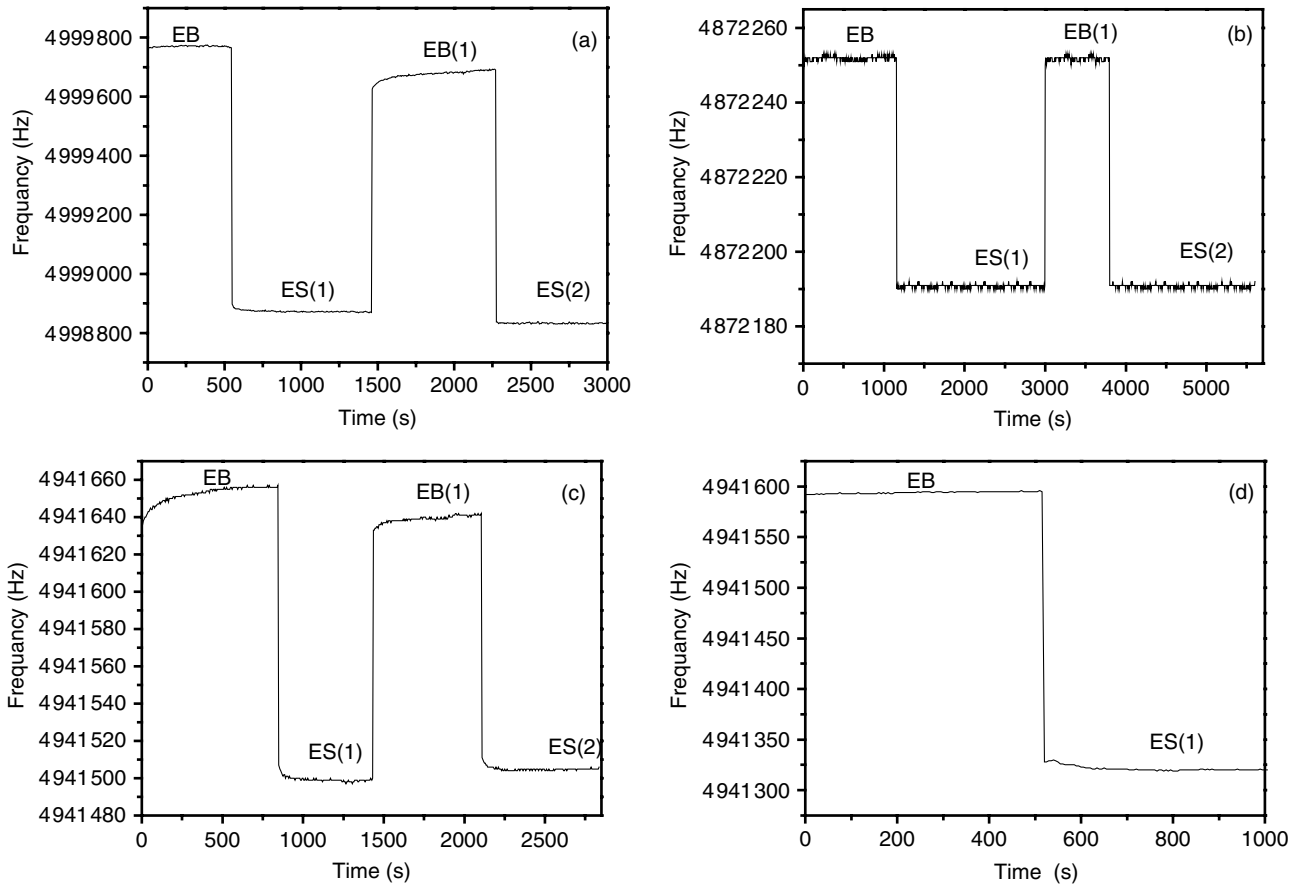

Figure 2. Subsequent redoping cycles in different acids: (a) 0.1 M sulfuric, (b) 0.1 M hydrochloric, (c) 0.1 M phosphoric and (d) 0.5 M trichloroacetic acids.

Table 1. The calculated wt.% values in different acids.

Dopant	Acid concentration ($mol\,l^{-1}$)	wt.% from first redoping cycle	wt.% from second redoping cycle	wt.% [a]
H_2SO_4	0.1	20	19	21.3
HC1	0.1	16.2	13	16.7
H_3PO_4	0.1	25.3	22.04	21.3
Cl_3CCOOH	0.5	33.9	–	45.7
CH_3COOH	0.1	11.63	13.7	
	0.5	36.6	27.11	
				24.9
	1.0	44.97	36.4	
	2.0	55.42	38.7	

[a] Calculated from the formula $C_{24}H_{20}N_4(A^-)_2$.

Similar experiments were carried out using hydrochloric, phosphoric and trichloroacetic acids instead of sulfuric acid, as shown in figures 2(b)–(d), respectively. In trichloroacetic acid, only one cycle of the redoping process was performed. A frequency change with time during redoping occurred immediately upon immersion in the acid solutions. The values of ***w*** during these cycles were calculated and are given in table 1. The values of ***w*** for hydrochloric and phosphoric acids indicate the presence of chloride and phosphate counter ions (scheme 1(b), $A^- = Cl^-$ and $1/2HPO_4^{2-}$, respectively). These values are very close to the ones obtained experimentally and those based on the molecular formula ($C_{24}H_{20}N_4A_2$, scheme 1(b)) for 50% intrinsically oxidized EB film after doping the imine sites [20, 32–35]. Redoping with trichloroacetic acid gives a value of ***w*** equal to 33.9 wt.%, which is small in comparison with the value based on the previous formula (45.7 wt.%) but very close to the value of 33 wt.% obtained by Wei and Hsueh [32] by thermal analysis when EB was doped with 0.5 M trichloroacetic acid. This could be attributed to the insufficient acid available to dope the imine sites.

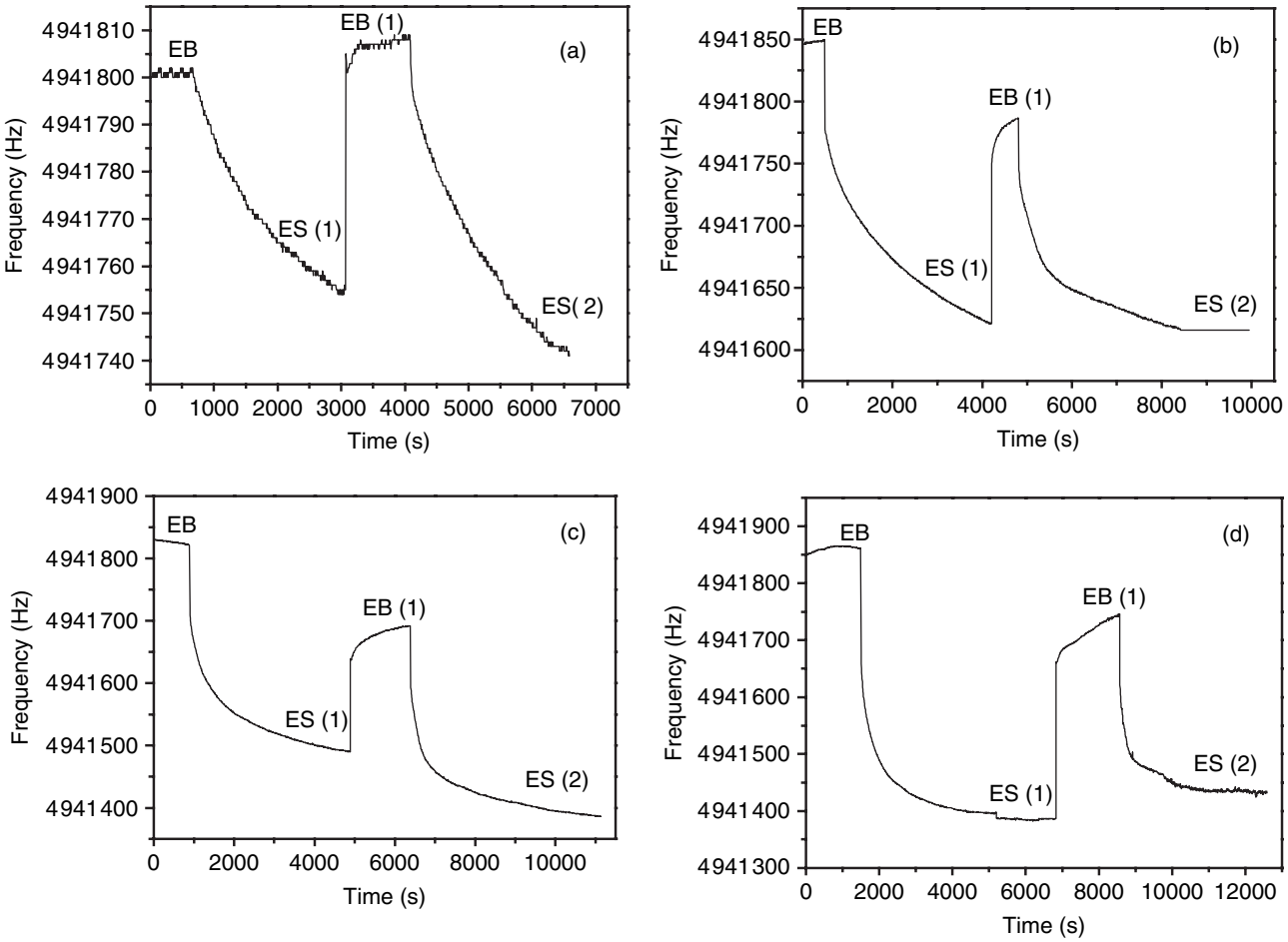

Figure 3. Redoping cycles in different acetic acid concentrations: (a) 0.1, (b) 0.5, (c) 1 and (d) 2 M.

3.2. Doping of PANI in acetic acid

The ability of the anion and proton of an acid to interact with PANI is related to the relative strength of the acid and to the amine and imine groups within the polymer. The p$K_a$values for the two acidic nitrogen groups within PANI have been determined by titration with NaOH [36]. They are 2.5 and 5.5 for ($-NH_2^+-$) and ($-NH^+=$), respectively. On the basis of these values, a strong acid (p$K_a < 2.5$) will protonate both groups. However, an acid with an intermediate pK_a value ($2.5 < pK_a < 5.5$) should result in the protonation of only the imine group. Since the pK_a of acetic acid is 4.7, it is sufficiently strong to protonate the imine group. It has been mentioned by Hatchett *et al* [37] on the basis of voltammetric and spectroscopic techniques that the pK_a of the acid affects the degree of doping of PANI and its redox state. The doping properties of PANI with weak acids such as acetic acid show different behavior than that of PANI doped with strong acids. Anion and proton doping is poor for the relatively weak acetic acid.

To trace the doping process, the time course for the frequency of the EB film was measured in 0.1, 0.5, 1 and 2 M solutions of aqueous acetic acid. Figure 3 shows plots of the frequency changes against time during the doping of different EB films. It is shown that the uptake of the dopant ions during the redoping process with acetic acid is different from that with strong acids. Doping with 0.1 M acetic acid increases exponentially with time until it reaches a steady state. However, doping with 0.5–2 M acetic acid occurs in two stages: rapid doping followed by an exponentially increases with time. This process ends with the PANI films doped with acetic acid ions (ES(1)). The films doped with 0.5–2 M acetic acid were dedoped with 0.1 M ammonia solutions. A second cycle of redoping with 0.1, 0.5, 1 and 2 M acetic acid was carried out to give the corresponding ES(2) films, which showed similar behaviors to the previous cycle. Also, it can be seen that the frequency change due to the rapid doping in the first redoping cycle is larger than that in the second cycle. For example in 0.5 M acetic acid, the frequency changes due to the rapid doping were 82 and 64 Hz in the first and second cycles, respectively.

The values of $\boldsymbol{w}$ for 0.1–2 M acetic acid were calculated as mentioned in the previous section and are given in table 1. It can be seen that $\boldsymbol{w}$ increases as the acid concentration increases. In addition, the values calculated for the first redoping cycle are larger those ones calculated for the second cycle except for 0.1 M acetic acid. The latter has approximately similar $\boldsymbol{w}$ values.

The structure of the polymer doped with acetic acid can be represented as scheme 1(b), where A is the acetate anion (Ac^-). For the molecular formula of 50% intrinsically

oxidized EB film after doping the imine sites with acetic acid to be $C_{24}H_{20}N_4(Ac)_2$ [34], w must be 24.9 wt.%. In the present work, doping EB film with 0.1 M acetic acid gives a value of w of 11.63%, however doping with 0.5 and 1 M acetic acid gives w= 36.6 and 44.5%, respectively. These values exceed the value obtained from the previously given formula (24.9 wt.%). A primary explanation for this may be that as the acid concentration increases, w increases and the doping of amine sites occurs, in addition to the doping of imine sites, as shown in schemes 1(c) and (d). Doping with 2 M acetic acid gives w= 55.42%, which exceeds the value of 48.8 wt.% obtained when all the imine and amine sites are doped with acetic acid ions ($C_{24}H_{20}N_4(Ac)_4$). However, when we consider doping EB in 1 M sulfuric acid, which is a strong acid, only the imine sites are doped. The molecular formula for 50% intrinsically oxidized EB film after doping is $C_{24}H_{20}N_4(HSO_4^-)_2$, and hence w approximately equals 35% [20, 32]. For comparison, the amount of acetic acid ($pK_a = 4.7$) needed to dope the polymer with the same number of protons would be on the order of 10^4 times higher than that of sulfuric acid. Therefore, the explanation for the calculated values of w for doping with 0.5 and 1 M acetic acid based on the doping of amine sites in addition to imine sites is not valid. Moreover, the higher value of w in the case of doping the EB film in 2 M acetic acid requires explanation.

It is reasonable to explain the values of w on the basis of the fact that acetic acid is a weak acid. During anion and proton doping in the PANI film, a significantly higher concentration of undissociated weak acid is needed inside the polymer to satisfy the charge neutrality. For each acetate anion doped in the polymer, $10^{4.7}$ undissociated molecules of acetic acid must associate with the polymer. Hence, a significant amount of undissociated acetic acid must be present in the polymer. Therefore, the high value of w in the case of 2 M acetic acid may be due to the possibility of the specific absorption and adsorption of acetic acid molecules in addition to the acid ions into the PANI film. This possibility also cannot be excluded in the cases of doping with 0.1, 0.5 and 1 M acetic acid. This is unlikely to occur during doping with 0.1 M acetic acid but becomes increasingly likely as the acid concentration increases. This hypothesis and the differences between w values calculated for the two cycles of redoping will be explained in the next section by the kinetic diffusion of acetic acid ions into the polymer film during the doping process.

3.3. Kinetics of dopant diffusion

The diffusion of small molecules through a polymer is an important phenomenon in many areas of science and engineering. For example, the diffusivity in polymer films and membranes [38, 39] is important in connection with the use of polymers as barrier coatings in packaging applications [40] and for separation-science applications [38, 41].

The study of the doping of acetic acid into PANI film in the form of EB involves both the equilibrium uptake and the kinetics of the doping process. The frequency changes with time during the doping processes indicating that the ion uptake, and hence the doping process, follows a slow diffusion process. The diffusion coefficient D of acetate and proton ions in addition to that of acid molecules into PANI films can be derived from gravimetric measurements. The mass uptake of a polymer film of thickness L can be obtained as a function of time during the transient regime. The mass uptake of the film can be determined from the change in the resonance frequency using the Sauerbrey equation. This is based on the fact that the frequency shift Δf during the doping process is related to the change in mass Δm. Suppose that Δf_t is the frequency change due to the doping of acetic acid at any time t and Δf_∞ is the frequency change in the equilibrium state at the end of the doping process, these two parameters can be given as follows:

$$\Delta f_t = f_{EB} - f_t \quad \text{and} \quad \Delta f_\infty = f_{EB} - f_\infty,$$

where f_t is the frequency during the doping process at time t, f_∞ is the frequency in the equilibrium state and f_{EB} is the frequency of the EB film. The frequency change ($\Delta f_t/\Delta f_\infty$) corresponds to ($\Delta m_t/\Delta m_\infty$) at the same time, where Δm_t is the polymer uptake at time t and Δm_∞ is the final polymer uptake.

Analysis of the obtained experimental data was based on solving Fick's second equation which has been reviewed by Crank [42]. As a typical example, the average value for D can be obtained from a plot of $\Delta f_t/\Delta f_\infty$ as a function of $t^{1/2}/L$. D can be calculated from the initial linear portion of the diffusion using

$$\frac{\Delta f_t}{\Delta f_\infty} = 4\sqrt{\frac{D}{\pi}}\frac{t^{1/2}}{L}. \qquad (2)$$

The relation between ($\Delta f_t/\Delta f_\infty$)and $t^{1/2}/L$ for different acetic acid concentrations suggests that the diffusion process follows Fickian kinetics and that the dopant undergoes the diffusion process [42]. The plots are linear for at least the first half of the curve, as shown in figure 4. For doping with 0.1 M acetic acid, the plot has a zero intercept with the time axis. In the cases of 0.5, 1 and 2 M acetic acid, similar behaviors were obtained except for at the early stage of the doping; the plots have a nonzero intercept with the time axis. This may be because surface diffusion and the adsorption of acetic acid molecules take place onto the surface of the PANI film, which occurred during the rapid doping stage. This would explain our previous observation at the first stage of doping EB film with 0.5, 1 and 2 M acetic acid. At the end of the surface diffusion, the acetic acid molecules and ions start to diffuse into the bulk and undergo volume diffusion.

The values of D were calculated for the two cycles of redoping and are given in table 2. They are in the range of $(0.076–1.64) \times 10^{-15}$ cm^2 s^{-1} and are reasonably similar to the rate of diffusion of organic molecules in a swollen polymer electrolyte [43]. It can be seen that D for the first cycle of redoping is smaller than the value calculated for the second cycle.

Kang *et al* [44] have quantitatively evaluated the effects of dedoping-redoping cycles on the surface intrinsic oxidation state ratios of EB films by x-ray photoelectron spectroscopy. The oxidation states of EB films were substantially enhanced

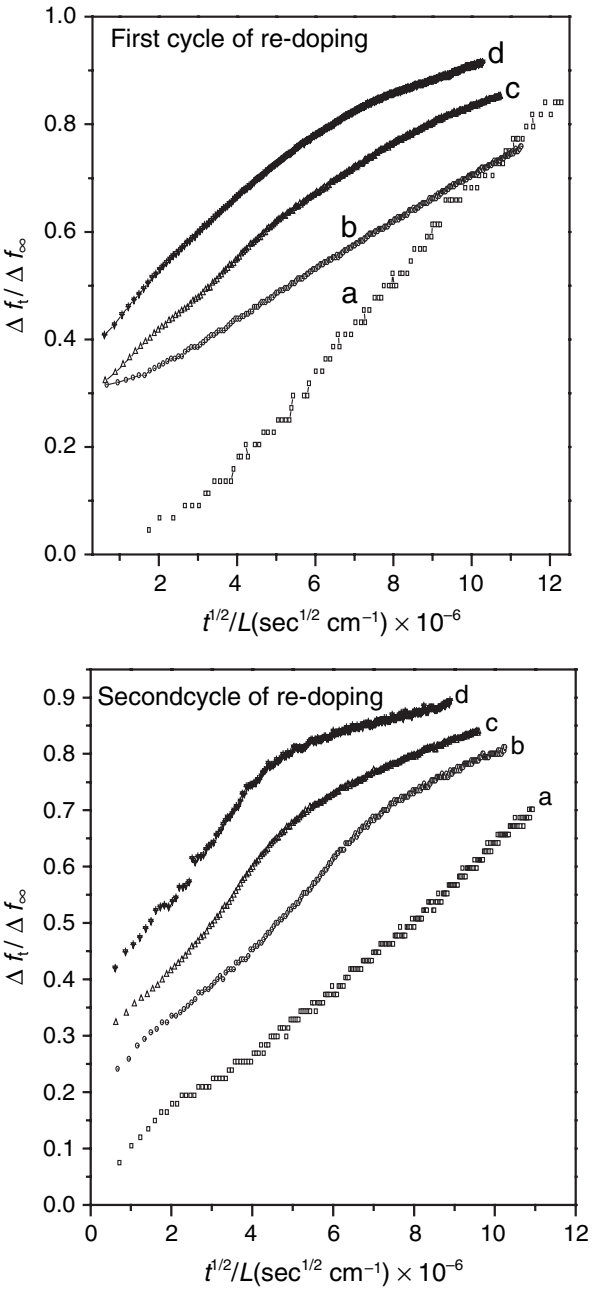

Figure 4. $\Delta f_t/\Delta f_\infty$ as a function of $t^{1/2}/L$ at different acetic acid concentrations for the two redoping cycles: (a) 0.1, (b) 0.5, (c) 1 and (d) 2 M.

during these cycles, particularly when high protonic acids were used. This behavior was explained in terms of the morphology-related diffusion limitations and the extent of the hydrolysis reaction. However, Hatchett *et al* [37] concluded that PANI is further reduced, and hence the oxidation states decrease, when it doped with a weak acid such as acetic acid. The latter phenomena, not only enhances the diffusion of the dopant ions and hence a larger D is obtained, but also decreases $\boldsymbol{w}$ for the second cycle of redoping. Also, Min *et al* [45] obtained different UV–Vis-near-infrared spectra during the dedoping–redoping cycle for PANI films depending on the type of acid used. These differences were attributed to conformational changes in the PANI chains during these

Table 2. D of different concentration of acetic acid ions in EB film during two cycles of redoping processes using QCM and UV–visible spectroscopy measurements.

$D \times 10^{15}(\mathrm{cm^2\ s^{-1}})$			
UV-visible measurement	QCM measurement	Redoping cycle	Acetic acid ($\mathrm{mol\,l^{-1}}$)
0.27	1.2	1	
			0.1
–	0.8	2	
0.12	0.312	1	
			0.5
–	0.252	2	
0.076	0.7	1	
			1.0
–	1.35	2	
0.205	0.736	1	
			2.0
–	1.64	2	

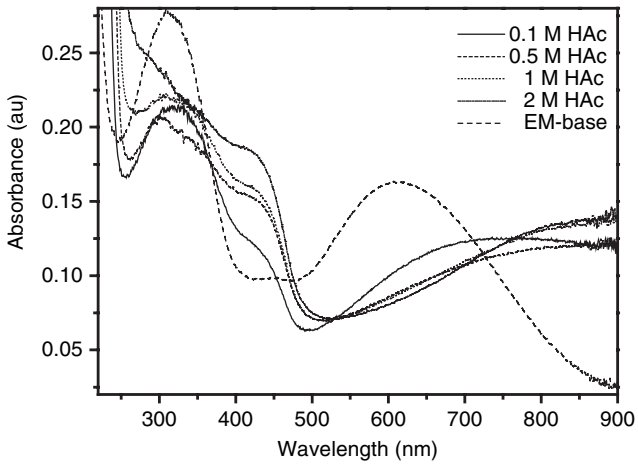

Figure 5. UV–Vis absorption spectroscopy after 60 min of redoping EB in different acetic acid concentrations.

cycles from a tight coil to an expanded coil [44, 45]. The acetate and proton ions may diffuse more easily into the core of the expanded coil, resulting in a higher value of D.

The second method we used for determining D for acetic acid ion diffusing into the PANI film was UV–Vis absorption spectroscopy. ES films were deposited onto the inner walls of quartz cuvettes. These films were dedoped in 0.1 M ammonia solution and then redoped in 0.1, 0.5, 1 and 2 M acetic acid. The UV–Vis absorption spectra for the EB films and ES films after 60 min of the redoping process were measured, as shown in figure 5. The spectra of the EB films exhibit characteristic bands at 314 and 620 nm, which are assigned to the π–π^* transition of the benzenoid rings and the molecular exciton associated with the quinine diimine structure, respectively. The absorption at 620 and 314 nm decreases on doping with acetic acid solution. The maximum absorption (λ_{max}) at ∼730 nm increases with time t. This new absorption is attributed to a bipolaron transition band due to the doping. This absorption diminishes with the formation of ES films, which exhibit a characteristic band at 425 nm and an extended band at wavelength larger than 730 nm. Both bands increase in intensity with time.

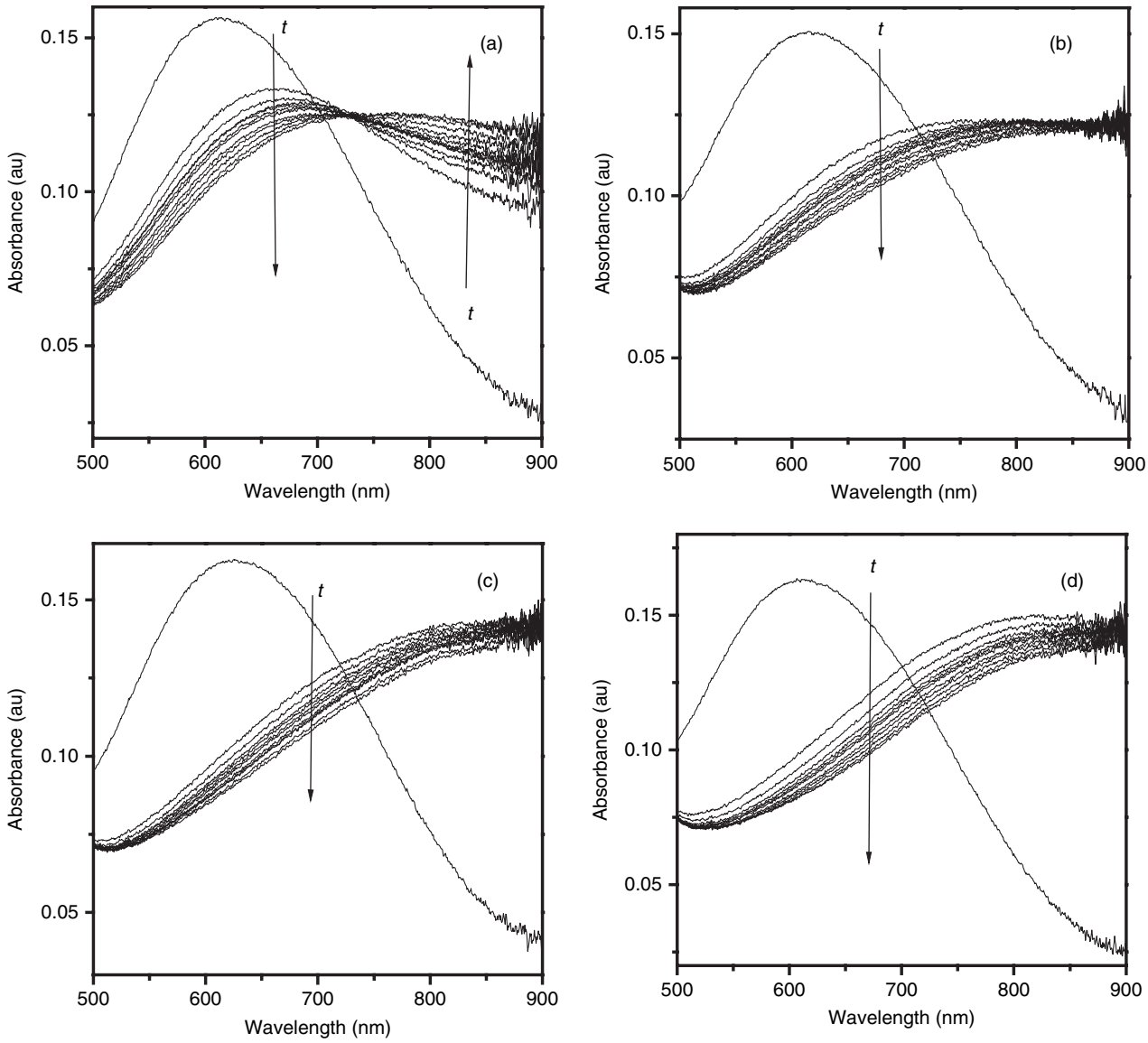

Figure 6. UV–Vis absorption spectroscopy at different times during the redoping of EB in different acetic acid concentrations: (a) 0.1, (b) 0.5, (c) 1 and (d) 2 M.

When the spectra were recorded over time, three isosbestic points were formed at 730, ∼473 and ∼363 nm when 0.1 M acetic acid was used for redoping (these spectra are not shown). The latter two points were seen during redoping with 1 and 2 M acetic acid. This is attributed to the equilibrium state existing between the EB and ES forms. The isosbestic point appearing at 730 nm for 0.1 M acetic acid was red shifted when 0.5 M acid was used. At a higher concentration of acetic acid, it is expected that the bipolaron transition band related to these ES films is absorbed in the near-infrared region.

These spectroscopic observations allow the analysis of the kinetic doping reaction. Figures 6(a)–(d) show the time course (t) of the UV–Vis spectra of the EB film in the region 600–900 nm for different concentrations of acetic acid solution. The $\Delta A_t/\Delta A_\infty$ ratios at 680 nm, which correspond to $\Delta M_t/\Delta M_\infty$, were calculated. ΔA_t is the absorbance change with respect to the absorbance of the EB film at time t and ΔA_∞ is the absorbance change in the equilibrium state at the end of the doping process (60 min) with respect to the absorbance of the EB film. These two parameters can be given as follows:

$$\Delta A_t = A_{EB} - A_t \quad \text{and} \quad \Delta A_\infty = A_{EB} - A_\infty,$$

where A_t is the absorbance during the doping process at time t, A_∞ is the absorbance in the equilibrium state and A_{EB} is the absorbance of the EB film.

The relation between $\Delta A_t/\Delta A_\infty$ and $t^{1/2}/L$ is shown in figure 7. It is clear that the doping reaction was controlled by a diffusion process [42, 46]. The values of D were calculated from the slopes of the initial plots, and are given in table 2. D is in the range $(0.076–0.27) \times 10^{-15}\,\mathrm{cm^2\,s^{-1}}$, which is slightly lower than the corresponding range obtained from the QCM measurements but still represents a feasible range of values [43].

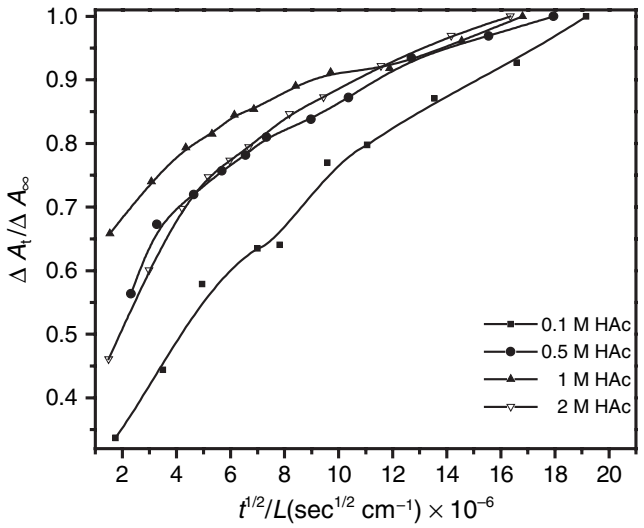

Figure 7. $\Delta A_t/\Delta A_\infty$ as a function of $t^{1/2}/L$ at different acetic acid concentrations during redoping in EB films.

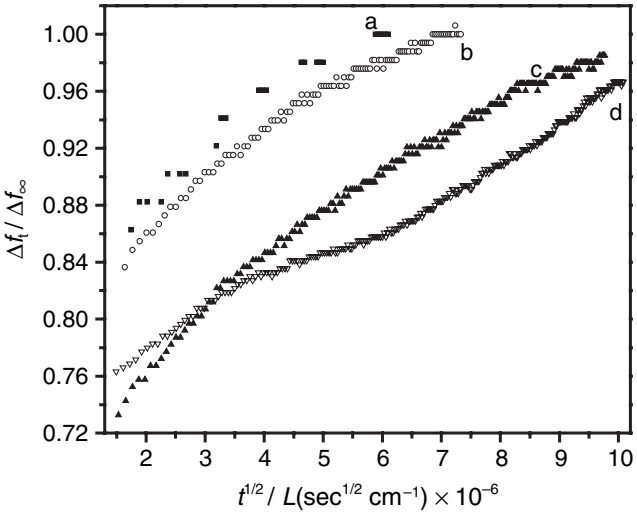

Figure 8. $\Delta f_t/\Delta f_\infty$ as a function of $t^{1/2}/L$ during the dedoping of different ES(1) films with 0.1 M ammonia.

3.4. Kinetics of dedoping diffusion

The frequency changes during the dedoping of different ES(1) films obtained from 0.1, 0.5, 1 and 2 M acetic acid with 0.1 M ammonia solution to produce the corresponding EB(1) films are shown in figure 4. It is clear that the expulsion process of dopant ions during the dedoping process is different from that with strong acids. The dedoping occurred in two stages: rapid dedoping followed by dedoping at a rate that decreases exponentially with time.

The kinetics of dedoping can be determined from the change in the resonance frequency with time. If Δf_t is the frequency change due to the dedoping of acetic acid at time t and Δf_∞ is the frequency change at the end of the dedoping process, these two parameters can be given as follows:

$$\Delta f_t = f_{ES} - f_t \quad \text{and} \quad \Delta f_\infty = f_{ES} - f_\infty,$$

where f_t is the frequency during the dedoping process at time t, f_∞ is the frequency at the end of the dedoping process and f_{ES} is the frequency of the ES film. Plots of $\Delta f_t/\Delta f_\infty$ as a function of $t^{1/2}/L$ are shown in figure 8. The relations follow Fickian kinetics and the dopant undergoes the diffusion process. The plots are linear for at least the first half of the curve and have a nonzero intercept with the time axis. This is due to the adsorption of acetic acid molecules taking place on the surface of the PANI film, which dedoped rapidly, and explains our previous observations during the redoping of EB films in 0.5, 1 and 2 M acetic acid. After the expulsion of the surface dopant, the diffusion of the expelled acetic acid molecules and ions starts at the bulk of the EB film. The values of D were calculated and are given in table 3. It can be seen that D for acetic acid expulsion is lower than D for the acid ion uptake.

Table 3. D of acetic acid during the dedoping processes of ES films using 0.1 M ammonia.

$D \times 10^{15}$ ($cm^2\ s^{-1}$)	Acetic acid ($mol\ l^{-1}$)
0.024	0.1
0.16	0.5
0.124	1.0
0.106	2.0

4. Conclusions

A QCM has been successfully used to monitor the formation of PANI films on the electrode of the quartz crystal during the oxidation of aniline. In this paper, we demonstrate that a QCM can also be used to characterize the dedoping and redoping processes in PANI. Also, it has been shown that there is a fundamental difference between the doping of PANI in strong and weak acids.

In 0.1 M strong acid, the doping of EB film is rapid; however, in acetic acid solution, the doping obeys Fickian diffusion kinetics. The present concept of the change in the crystal frequency as a result of the mass increase or decrease during the doping or dedoping of PANI, respectively, was used in the determination of the type of diffusion and its coefficient. It was concluded that the diffusion depends on the morphology and the oxidation state of the EB film.

References

[1] Skotheim T A 1986 *Handbook of Conducting Polymers* vols 1 and 2 (New York: Marcel Dekker)
[2] MacDiarmid A G, Mu S L, Somasiri N L D and Wu W 1985 *Mol. Cryst. Liq. Cryst.* **121** 187
[3] Novak P, Muller K, Santhanam K S V and Hass O 1997 *Chem. Rev.* **97** 207
[4] Kobayashi T, Yonevama N and Tamura H 1984 *J. Electroanal. Chem.* **177** 281
[5] Batich C D, Laitinen H A and Zhou H C 1990 *J. Electroanal. Soc.* **137** 883
[6] Desilvestro J and Hass O 1985 *J. Chem. Soc. Chem. Commun.* **346**
[7] Dong Y H and Mu S L 1991 *Electrochim. Acta* **36** 2015

[8] Karg S, Scott J C, Salem J R and Angelopoulos M 1996 *Synth. Met.* **80** 111
[9] Bartlett P N and Whitaker R G 1987/1988 *Biosensor* **3** 359
[10] Yang Y F and Mu S L 1997 *J. Electroanal. Chem.* **432** 71
[11] Gospodinova N and Terlemezyan L 1998 *Prog. Polym. Sci.* **23** 1443
[12] Skotheim T A, Elsenbaumer R L and Reynolds J R 1998 *Handbook of Conducting Polymers*, 2nd edn (New York: Marcel Dekker)
[13] Huang W S and MacDiarmid A G 1993 *Polymer* **34** 1833
[14] Kang E T, Neoh K G and Tan K L 1998 *Prog. Polym. Sci.* **23** 277
[15] Stafström S, Bredas J L, Epstein A J, Woo H S, Tanner D B and MacDiarmid A G 1987 *Phys. Rev. Lett.* **59** 1464
[16] Focke W W, Wnek G E and Wei Y 1987 *J. Phys. Chem.* **91** 5813
[17] Wang V and Rubnev M F 1992 *Synth. Met.* **47** 255
[18] Morales G M, Miras M C and Barbero C 1999 *Synth. Met.* **101** 686
[19] Nunziante P and Pistoia G 1989 *Electrochim. Acta* **34** 223
[20] Ayad M M, Zaki E A and Stejskal J 2007 *Thin Solid Films* **515** 8381
[21] Chiang J and MacDiarmid A G 1986 *Synth. Met.* **13** 193
[22] Kang E T, Neoh K G and Tan K L 1995 *Synth. Met.* **68** 41
[23] Ayad M M 1994 *J. Appl. Polym. Sci.* **53** 1331
[24] Ayad M M 1994 *J. Polym. Sci. Polym. Chem.* **32** 9
[25] Ayad M M 1994 *Polym. Int.* **35** 35
[26] Sauerbrey G 1959 *Z. Phys.* **155** 206
[27] Nomura T and Iijima M 1981 *Anal. Chim. Acta* **131** 97
[28] Kanazawa K K and Gordon J G 1985 *Anal. Chem.* **57** 1770
[29] Ebara Y and Okahata Y 1994 *J. Am. Chem. Soc.* **116** 11209
[30] Sato T, Serizawa T and Okahata Y 1996 *Biochim. Biophys. Acta* **1285** 14
[31] Ayad M M and Shenashin M A 2003 *J. Eur. Polym.* **39** 1319
[32] Wei Y and Hsueh K F 1989 *J. Polym. Sci. A: Polym. Chem.* **27** 4351
[33] Kang E T, Neoh K G, Khor S H, Tan K L and Tan B T G 1989 *J. Chem. Soc., Chem. Commun.* **11** 695
[34] Tan K L, Tan B T G, Kang E T and Neoh K G 1989 *Phys. Rev.* B **39** 8070
[35] Blinova N V, Stejskal J, Trchová M and Prokeš J 2006 *Polymer* **47** 42
[36] Menardo C, Nechtschein M, Rousseau A, Travers J P and Hany P 1988 *Synth. Met.* **25** 311
[37] Hatchett D W, Josowicz M and Janata J 1999 *J. Phys. Chem.* B **103** 10992
[38] Veith W R 1991 *Diffusion in and through Polymers: Principles and Application* (New York: Oxford University Press)
[39] Mark J E 1996 *Physical Properties of Polymers Handbook* (New York: American Institute of Physics)
[40] Strandburg G, DeLassus P T and Howell B A 1990 *ACS Symposium series* vol 423, ed W J Koros (Washington: American Chemical Society) p 333
[41] Rangarajan R, Matsuura T and Sourirajan S 1985 *Reverse Osmosis and Ultrafiltration (ACS Symposium series vol 281)* (Washington: American Chemical Society)
[42] Crank J 1975 *The Mathematics of Diffusion* 2nd edn (Oxford: Clarendon) p 414
[43] Vogt B D, Soles C L, Lee H J, Lin E K and Wu W I 2004 *Langmuir* **20** 1453
[44] Kang E T, Li Z F, Neoh K G, Dong Y Q and Tan K L 1998 *Synth. Met.* **92** 167
[45] Min Y, Xia Y, MacDiarmid A G and Epstein A 1995 *Synth. Met.* **69** 159
[46] Yamamoto K, Yamada M and Nishiumi T 2000 *Polym. Adv. Technol.* **11** 710